Distribution of Prompt-Neutron Emission Probability for the Fission Fragments of U^{233}

J. S. FRASER AND J. C. D. MILTON
Chalk River Laboratory, Atomic Energy of Canada Limited, Chalk River, Ontario
(Received November 13, 1953)

The kinetic energies of both members of coincident fragment pairs were measured in a double back-to-back grid ionization chamber. The pulse heights were recorded only when coincident with a prompt fast neutron detected in either one of two neutron counters placed on opposite sides of the fission chamber. The strong angular correlation of the direction of motion of the prompt fission neutrons with the direction of motion of the emitting fragment permitted the identification of the latter as the emitting fragment. The frequency distributions of modes obtained by gating with a neutron from the light or from the heavy fragment were compared with the distribution recorded without a neutron coincidence. Comparison of the three sets of data show (1) that neutron emission from the light fragment predominates at low mass ratios, whereas at high mass ratios neutron emission from the heavy fragment is more probable; (2) that a broad maximum in the total neutron yield exists in the region of the most probable fission mode; and (3) that the average total kinetic energy curve is essentially the same for the three conditions of measurement.

I. INTRODUCTION

A STUDY of the angular distribution of the prompt fission neutrons[1] has shown that on the average the light-fragment group emits 30 percent more neutrons than does the heavy. The present experiment was undertaken to examine in more detail the distribution of prompt-neutron emission probability among the various fission modes.

A "fission mode," as used here, will be defined by the kinetic energies of the two fragments, so that a measurement of the distribution of these energy pairs in coincidence with a prompt neutron is required. The neutron-emitting fragment may be identified as a result of the strong correlation of the direction of motion of the neutron in the laboratory system with the direction of the fragment. If the coincident fragment pairs are collimated and the neutron detector placed on the axis of the collimator, the probability of detecting a neutron from a fragment receding from the neutron counter is completely negligible compared with that for a fragment approaching it.[1] To increase the counting rate, two neutron counters were used, one on each side of the fission chamber. The neutron-emitting fragment was identified as the one approaching the counter which detected the neutron.

II. EXPERIMENTAL ARRANGEMENT

The detectors and their associated electronic circuits are depicted schematically in Fig. 1. The fission chamber is a double back-to-back grid ionization chamber employing electron collection. The thin fissile source of 2 $\mu g/cm^2$ of U^{233} is contained in a collodion film approximately 20 $\mu g/cm^2$. It was prepared after the manner described by Brunton and Hanna.[2] The film was laid on a 0.015-in. thick aluminum plate which had been drilled with an array of equidistant 0.030-in. diameter holes. Over this was placed a similar plate with matching holes. Thus, the fragments were collimated on both sides; the maximum angle of emission of a pair of fragments was 45° from the normal, the most probable angle of emission being about half of this value. As two coincident fragments move very nearly, if not precisely, in opposite directions, a collimator is required on only one side of the source. The second plate was used to minimize the number of noncoincident fragments.

The single counting rate of fission fragment pulses, nearly equal in the two chambers, was approximately 3000 per minute. The rate of counting coincident pairs was about 1100 per minute.

The source was mounted in the grounded cathode common to the two chambers. The grid-cathode spacing was 3.0 cm and the collector was spaced 1.0 cm from the grid. The grid was wound on a brass frame with 0.008-in. diameter nickel wire spaced 0.10 in. center-to-center. According to the theory of Buneman, Cranshaw, and Harvey,[3] this provides a screening of the collector from positive-ion induction of 96 percent efficiency.

The chamber was filled by first admitting 1.5 cm Hg of CO_2 and then argon until the total pressure was 100 cm Hg. Pulse-height saturation of the fission pulses was achieved with 1400 volts on the grid and 2800 volts on the collector. The ratio of the field strengths in grid-collector and cathode-grid regions was thus 3:1, which is adequate to reduce collection of electrons by the grid to a negligible value. The rise time of the pulses was about 0.3 μsec. The purity of gas filling was checked daily on a 30-channel kicksorter by comparing the fission pulse spectrum with pulses from a mercury-switch pulse generator stabilized by OD2 and 5651 regulator tubes in cascade. If the fission pulses drifted by more than one percent, the chamber was refilled.

The neutron counters used were methane-filled cylindrical ionization chambers. They were identical to the type described previously.[1]

Each of the four counters was connected to a preamplifier and provided with a 1-$\mu\mu$f condenser for coupling the signal generator pulses to the input grid. Each of

[1] J. S. Fraser, Phys. Rev. 88, 536 (1952).
[2] D. C. Brunton and G. C. Hanna, Can. J. Research A28, 190 (1950).
[3] Buneman, Cranshaw, and Harvey, Can. J. Research A27, 191 (1949).

the preamplifiers fed a linear amplifier and discriminator. The discriminator outputs of the two neutron counters were mixed together in a twin triode circuit with a common cathode resistor. The output of this circuit, together with the discriminator outputs from the two fission-chamber amplifiers were delay-line-shaped to rectangular pulses approximately 0.8 μsec wide and fed into a triple-coincidence circuit. In this manner a triple coincidence could be registered between a pair of fragments and a neutron in either one of the neutron counters.

The amplified output from each fission chamber was transformed into a flat-topped pulse 15 μsec wide with amplitude proportional to the fission pulse.[2] When a triple coincidence occurred, a gate pulse was generated which allowed a 5-μsec wide portion of the flat-topped pulses to pass to two-stage pulse-lengthening circuits.[4] These produced pulses 3 sec long to deflect the pens of two synchronized Esterline-Angus recording milliammeters. The triple coincidence gate pulse also allowed the appropriate neutron pulse to actuate an operation recorder pen on the edge of that chart associated with the neutron-emitting fragment. The record of an event thus consisted of the pen deflections proportional to the ionization energies of the pair of fragments and a side pen deflection indicating the neutron-emitting fragment.

The energy range was divided arbitrarily into 50 channels by the chart scale. The channel width was 2.75 Mev. The linearity and zero of the complete system from preamplifier to chart was checked daily with the pulse generator. The pulse-lengthening circuits had a tendency to show a slow drift of the base line; in order to facilitate the rejection of any run in which a drift of half a channel or more occurred, the equipment was monitored automatically at regular intervals. It was arranged to have about 15 signal-generator pulses of fixed amplitude recorded on both charts during one minute of each hour. As the coincidence counting rate achieved was about 0.8 per min, no serious loss of true events resulted from the superposition of the monitoring signals.

At intervals throughout the course of the experiment the pulse-height spectra of coincident fragment pairs were recorded without reference to neutron emission. This was done by operating the gate pulse generator by the output of an auxiliary double-coincidence circuit whose resolving time was about 1 μsec. In order to get a large number of evenly spaced pulses on the charts, the fluctuation in the time intervals between pulses was reduced by scaling down the coincidence output by 100 before operating the gate generator. The scaler introduced a delay of 6 μsec between the amplified output and the gate; the peak voltmeter pulses were sufficiently flat, however, that no detectable difference was observed with the gate delayed by this amount.

The discriminator outputs of each of the neutron counters and one of the fission chambers were recorded on scalers.

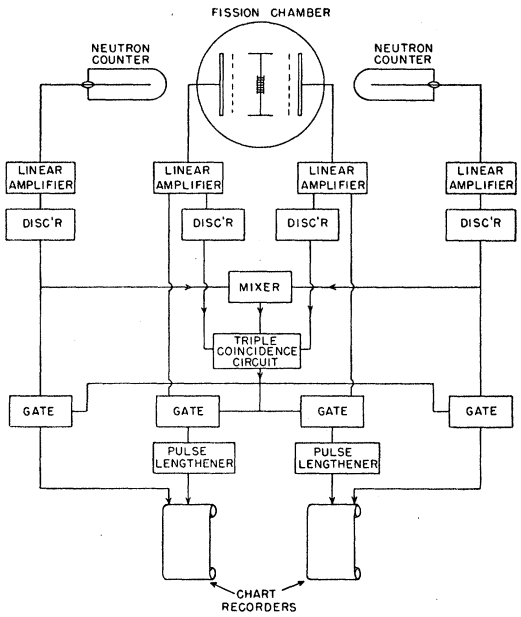

FIG. 1. Schematic diagram of the experimental equipment.

III. CORRECTIONS

Chance Events

The neutron coincidence data recorded on the charts are logically separated into two groups: (1) $N_L(E_L,E_H)$ with the neutron detected in the direction of motion of the light fragment, and (2) $N_H(E_L,E_H)$ with the neutron detected in the heavy-fragment direction. The results of all acceptable runs were thus separated and plotted as number of events on a grid with the light- and heavy-fragment channel numbers as coordinates. The third set of data is that taken without reference to neutron emission. This will be described as the normal distribution, $N_N(E_L,E_H)$.

The first two distributions of events must be corrected for the distribution of random events which comprised $\sim$6 percent of the total. The principal source of the random background was chance coincidences between a neutron count and a true fragment-fragment coincidence. The number of chance counts per minute was computed by taking the product of the resolving time, the sum of the two neutron counting rates and the known fraction of fission-chamber single counting rate which gave fragment-fragment coincidences. The resolving time was obtained by observing the rate of random coincidences between signal-generator pulses fed into one neutron-counter circuit and one of the fission-chamber outputs fed into the other two of the triple-coincidence inputs. The number of chance events is divided equally between the two groups, as there is no preference for the chance neutron count to be associated with either the light or the heavy fragment pulse

[4] J. T. Dewan and K. W. Allen, Rev. Sci. Instr. **21**, 823 (1950).

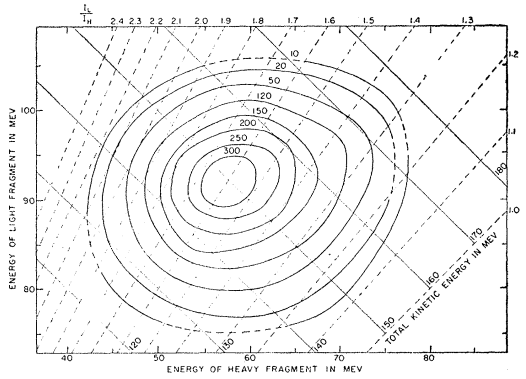

FIG. 2. Contour diagram of fission modes of U^{233} emitting neutrons from the light fragment. The solid lines are lines of constant total ionization. The dashed lines are lines of constant ionization ratio. The ionization ratio is only approximately proportional to the mass ratio M_H/M_L because of the ionization defect of fission fragments (reference 5). The energy scales have been corrected only for the neutron recoil effect and the source and collimator losses (see Sec. III) and not for ionization defect.

formed by a coincident pair. The distribution of the chance events on the coordinate grid is the same as $N_N(E_L,E_H)$. The number of random events, $B(E_L,E_H)$, at each point of the grid is thus computed from the relation $B(E_L,E_H)=\frac{1}{2}N_N(E_L,E_H)\times(B_{FF}/N_{FF})$ where B_{FF} is the total number of background counts, and N_{FF} is the total number in the normal distribution $N_N(E_L,E_H)$.

The random background in $N_N(E_L,E_H)$ is completely negligible. The number of chance fragment-fragment coincidences in the approximately 20 000 recorded events is only 4.

Neutron Recoil Correction

When a fragment emits a neutron, the change in the fragment energy is governed by the conservation of momentum. The assumption has been made that the neutron emission occurs after the fragments have separated. If the emission is assumed to be isotropic in the center-of-mass system and the recoil is averaged

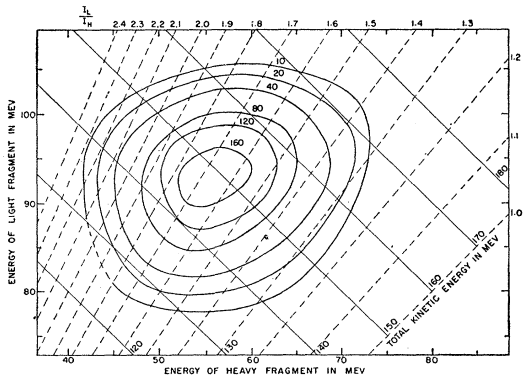

FIG. 3. Contour diagram of fission modes of U^{233} emitting neutrons from the heavy fragment. The energy scales have been corrected only for the neutron recoil effect and the source and collimator losses (see Sec. III) and not for ionization defect.

over all angles, the net reduction in kinetic energy of the fragment is equal to the kinetic energy of one neutron travelling with the velocity of the fragment. The average change in fragment energy ΔE_f is given approximately by $\langle\Delta E_f\rangle_{Av}=\frac{1}{2}M_nV_f^2$. This is the situation prevailing when the fragment energies are measured without reference to neutron emission, since the prompt-neutron emission occurs before the fragment has lost an appreciable amount of energy by ionization.[1]

In the present experiment where the fragment energies are measured in coincidence with a neutron, the range of angles of neutron emission is restricted by the geometry of the apparatus. In this case the average reduction of fragment energy is given by

$$\langle\Delta E_f\rangle_{Av}=\tfrac{1}{2}M_nV_f^2+V_f\langle p_n\cos\theta\rangle_{Av}, \quad (1)$$

where p_n is the momentum of the neutron and θ is the angle between the fragment's initial velocity and the neutron velocity, both p_n and θ being in the center-of-mass system. The average of $p_n\cos\theta$ is taken over the allowed range of angles θ. The details of the calculation and the assumptions involved are described in Appendix I. The results are given in Table I where the two terms of Eq. (1) are shown separately.

TABLE I. Values of $\frac{1}{2}M_nV_f^2$ and $V_f\langle p_n\cos\theta\rangle_{Av}$ in Mev.

	$\frac{1}{2}M_nV_f^2$	$V_f\langle p_n\cos\theta\rangle_{Av}$
Light fragment ($V_f=1.43\times10^9$ cm/sec)	2.12	0.87
Heavy fragment ($V_f=0.933\times10^9$ cm/sec)	0.90	0.80

The second term represents the difference in the energy of the fragment between the two conditions of measurement, *viz.*, with and without the detection of a coincident neutron.

The corrections were applied as follows: for the set of data in which the neutron was associated with the light fragment, 0.87 Mev was added to the measured values of the light-fragment energies; for the other set, 0.80 Mev was added to the heavy-fragment energies.

Ionization Defect Correction

The ionization defect of a fission fragment, which was measured by Leachman,[5] does not have a simple dependence on the energy of the fragment but is rather a function of the mass. No attempt was made to correct the contour diagrams of Figs. 2–6 for this effect. In Figs. 7–9, where the results are given in terms of mass ratios, an approximate correction has been applied to the ionization energy ratios to convert them to mass ratios. The ionization defect was assumed to have, for the sake of simplicity, the form $\Delta E=a+bM$, where a and b are constants and M the mass of the fragment. Using 5.7 and 6.7 Mev for defects of the most probable light and heavy fragments, respectively, gives $a=4.0$ Mev and $b=0.019$ Mev. Average values of 6.0 and 6.8

[5] R. B. Leachman, Phys. Rev. **87**, 444 (1952).

Mev, respectively, were used to correct the energy scales; the error introduced by assuming a constant value of the defect for each fragment group was ≤ 0.4 Mev over the whole range of modes.

Detection Efficiency Correction

Given an equal number of neutrons per fragment, the probability of detecting one from the light fragment is greater than detecting one from the heavy. The larger average velocity of the light fragment throws more neutrons into the cone of detection and at the same time raises the average neutron energy in the laboratory system. Both effects result in a greater detection efficiency for the light fragment. When making a quantitative comparison between the number of events in the two groups this was taken into account. It has not been corrected for in plotting the contours of Figs. 2 and 3.

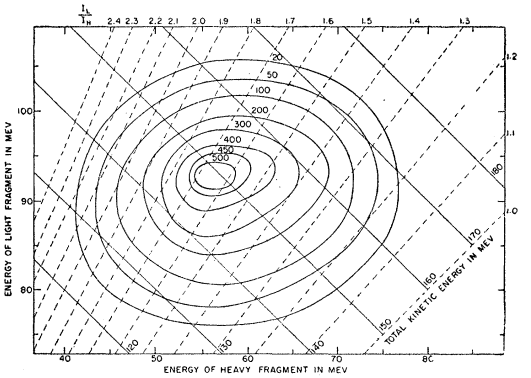

FIG. 4. Contour diagram of fission modes of U^{233} as measured without reference to neutron emission. The energy scales have been corrected only for the source and collimator losses (see Sec. III).

An approximate calculation,[1] which uses the average fragment velocities as measured by Leachman,[5] a reasonable neutron spectrum in the c.m. system, the measured counter efficiency curve, and isotropic neutron emission, yields a ratio $E_L/E_H=1.43$ for the two efficiencies.

Sources and Collimator Losses

The loss of energy in the source is almost entirely due to absorption in the 20-μg/cm^2 collodion film. Considering that the average fragment traverses slightly more than one-half of this thickness and assuming the rate of energy loss[6,7] as 0.058 Mev/(μg/cm^2) of collodion, one estimates an average energy loss of 0.6 Mev.

The collimator loss arises from the recombination of ions in the low field region inside the collimator holes. An average loss of 1.1 Mev was adopted on the basis of an approximate calculation of the field distribution in the holes and of measurement of the pulse-height saturation curve.

[6] N. O. Lassen, Kgl. Danske Videnskab. Selskab, Mat.-fys. Medd. **25**, 11 (1949).

[7] C. Wiegand and E. Segrè, U. S. Atomic Energy Commission Report MDDC-134 (unpublished).

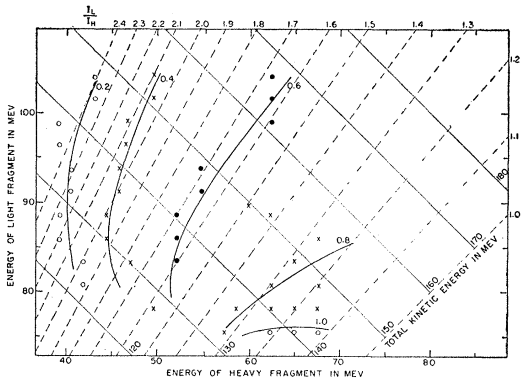

FIG. 5. Contours of constant relative probability per mode of neutron emission from the light fragment of U^{233}. The numbers adjacent to these contours are the ratios of the heights of the contours in Fig. 2 to those in Fig. 4.

IV. DISCUSSION OF RESULTS

The net numbers of neutron coincidence events recorded were 12 886 in group 1 (neutrons from light fragment), 7288 in group 2 (neutron from heavy fragment), and 19 481 in group 3 (no neutron coincidence required). The relative numbers in the first two groups are consistent with the ratio expected from the angular distribution of prompt neutrons[1] in U^{233} fission.

Contour diagrams of the fission modes for the three groups are given in Figs. 2–4. The contours are lines of constant frequency of occurrence. The numbers adjacent to the contours are interpolated from the net number recorded in a unit cell of the grid. The group 3 data, Fig. 4, are a remeasurement of the results obtained by Brunton and Hanna[2] for U^{233}. Substantial agreement of the present results with the earlier work is obtained.

The first two diagrams show distinct differences from the third. The peak in Fig. 2 is shifted towards a lower

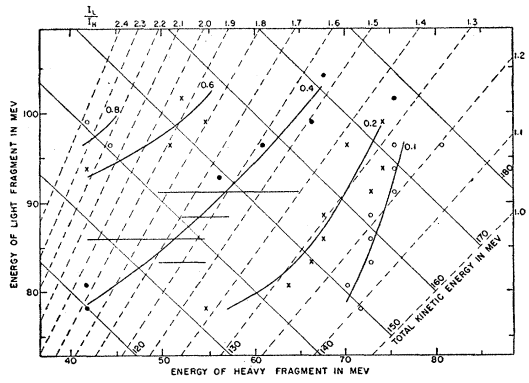

FIG. 6. Contours of constant relative probability per mode of neutron emission from the heavy fragment of U^{233}. The numbers adjacent to these contours are the ratios of the heights of the contours in Fig. 3 to those in Fig. 4. The horizontal bars on the contour labelled 0.4 indicate that the observed neutron emission probability is constant over the length of the bar.

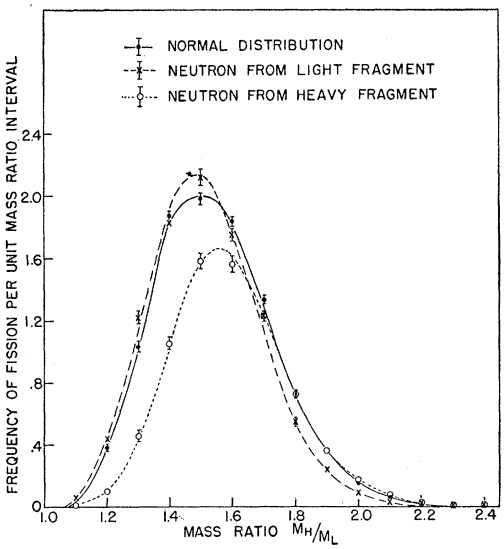

FIG. 7. Frequency of fission per unit mass ratio interval for the three groups of data. All of the corrections discussed in Sec. III have been applied in constructing the mass ratio scales of Figs. 7, 8, and 9.

mass ratio, whereas the peak in Fig. 3 is displaced to a higher mass ratio. In Figs. 2 and 3 one has, for a given light- and heavy-fragment energy, i.e., a given mode, a plot of neutron coincidences per unit time. The distribution taken without reference to neutron emission, which may be called the normal distribution, gives the relative frequency of occurrence for that mode. If one divides the coincidence distribution of, say, Fig. 2, by the normal distribution, one gets a number of proportional to the average number of neutrons emitted by the light fragment of that mode, and similarly for the heavy fragment distribution. Then one may construct in each case contours of constant neutron emission probability per mode. Such contours are shown in Figs. 5 and 6.

The interesting features of these diagrams are a variation of at least five to one and the strong correlation of the lines of constant probability with the mass ratio. When the neutron is emitted by the light fragment, the highest contours are in the region of low mass ratios. Conversely, when the neutron is emitted by the heavy fragment, the highest contours are in the region of high mass ratio.

These results may be summarized briefly by stating that neutrons are emitted predominantly by the heaviest light fragments and by the heaviest heavy fragments. This feature is also illustrated in plots of the frequency of fission as a function of the mass ratio. These functions have been calculated for the three groups of data by the method described in Appendix II. The energy scales were first corrected for neutron recoil, ionization defect, and source and collimator losses as described in Sec. III. The results are shown in Fig. 7. The relative areas under the curves of the neutron-fragment coincidence data have been adjusted for the relative neutron detection efficiency. It is evident that there is a mutual displacement of the curves parallel to the mass ratio axis. The curve for the neutron from the light fragment is at a lower mass ratio than the normal, whereas that for the neutron from the heavy fragment is displaced towards higher mass ratios.

It is of interest now to compare the relative frequency of neutron emission which one gets by dividing the ordinates of the coincidence curves in Fig. 7 by the corresponding ordinates of the normal curve. Curves A and B in Fig. 8 were obtained in this way. Curve A gives the relative neutron emission frequency for the heavy fragment and curve B the same for the light fragment. This shows in an even more striking way that neutron emission from the light fragment predominates at low mass ratios, whereas at high mass ratios emission from the heavy fragment is greater.

In a study of the neutron angular distribution[1] it was concluded that, on the average, there were 30 percent more neutrons from the light fragment than from the heavy. The distribution of mass ratios (the normal curve of Fig. 7) is such that mass ratios below the crossover of curves A and B are weighted more heavily than those above. An approximate value for the average neutron emission ratio for the light and heavy fragment groups is given by the ratio of the areas under the coincidence curves of Fig. 7. This ratio of 1.24 is consistent with the value 1.30 obtained with better angular resolution.[1]

Curve C of Fig. 8 is the sum of curves A and B and, therefore, represents the total neutron emission probability. There is evidently a broad maximum in the ν_R value (number of neutrons per fission with mass ratio R) in the mass ratio range 1.5 to 1.8. The departure from a constant total neutron yield is not large compared

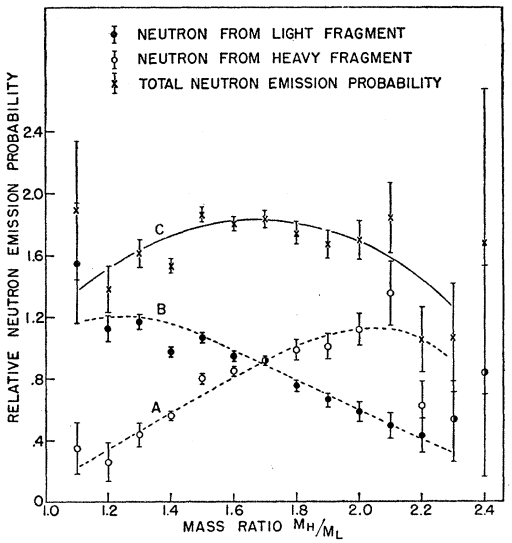

FIG. 8. Relative neutron emission probability as a function of mass ratio for the light and heavy fragments

with the variation exhibited for each fragment group. The predominant effect appears to be the change in neutron emission probability from one fragment group to the other as the mass ratio varies.

The average total kinetic energy for the three sets of data was calculated by the method described in Appendix II. No systematic difference in the three results is discernible in Fig. 9. All three show a significant maximum at a mass ratio of about 1.2. This is in agreement with the results obtained by Brunton and Hanna for the normal distribution.

ACKNOWLEDGMENTS

The authors wish to express their thanks to C. S. Scully and J. Kuehner for performing the rather laborious task of scanning the pulse analyzer records and to Miss A. R. Rutledge and Miss B. J. Sears for carrying out numerical computations. Discussions with Mr. G. C. Hanna, Dr. T. D. Newton and Dr. L. G. Elliott are gratefully acknowledged.

APPENDIX I

Calculation of the Recoil Correction

Figure 10 shows the vector relationships of the initial velocity V_i of the fragment, the final fragment velocity V_f, the fragment recoil velocity V_r in the c.m. system, and the velocity V_n of the neutron in the c.m. system. θ is the angle of neutron emission in the c.m. system relative to the initial direction of the fragment. The initial kinetic energy of the fragment may be written as $E_i=\frac{1}{2}(M+M_n)V_i^2$, where M is the mass of the final fragment and M_n is the neutron mass. The final energy

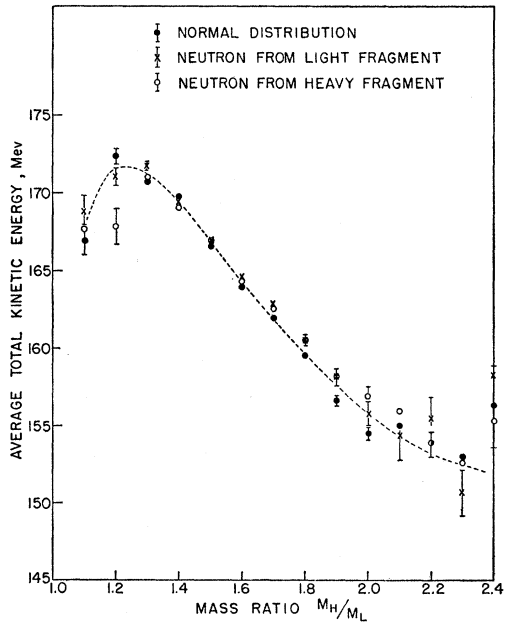

FIG. 9. Average total kinetic energy as a function of the mass ratio for the three groups of data.

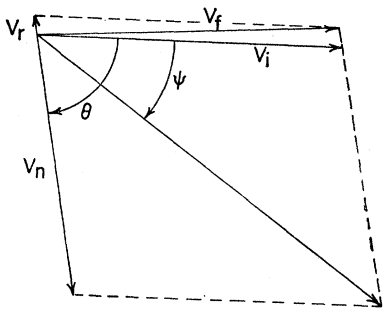

FIG. 10. Fragment and neutron velocity relationships.

of the fragment is

$$E_f=\tfrac{1}{2}MV_f^2=\tfrac{1}{2}M(V_i^2+V_r^2-2V_iV_r\cos\theta). \quad (2)$$

The decrease in fragment energy due to the emission of one neutron of velocity V_n at an angle θ is

$$\Delta E=E_i-E_f=\tfrac{1}{2}M_nV_i^2-\tfrac{1}{2}MV_r^2+MV_iV_r\cos\theta. \quad (3)$$

In the c.m. system, $MV_r=M_nV_n$, so that

$$\Delta E=\tfrac{1}{2}M_nV_i^2-\tfrac{1}{2}(M_n/M)M_nV_n^2+V_iM_nV_n\cos\theta. \quad (4)$$

The average values of V_n and V_i are of the same order, so that the second term may be neglected.

For a given value of V_i the average energy decrease is then

$$\langle\Delta E\rangle_{Av}=\tfrac{1}{2}M_nV_i^2+V_i\langle p_n\cos\theta\rangle_{Av}, \quad (5)$$

where p_n is the neutron momentum in the c.m. system.

When fragment energies are measured without reference to neutron emission, the second term is averaged over all values of θ, whence on the simplest assumption of an isotropic distribution, it becomes equal to zero. If, however, the energies are measured only in coincidence with a neutron detected inside a cone about the direction of motion of the fragment, $p_n\cos\theta$ is averaged only over the range of values of θ allowed by the geometry of the system.

In Fig. 11 the spherical triangle FAN is formed by the angle θ_c between the neutron's direction SN and the collimator axis SA, the angle η between the fragment's direction SF and the collimator axis, and the angle ψ between the neutron and fragment directions. The maximum value of η defined by the collimator was 45°. As the angular resolution of the neutron counter was considerably less than the angular spread introduced by the collimator, it is assumed in the following that its effect on the calculated value of $\langle p_n\cos\theta\rangle_{Av}$ is unimportant. In the measurements reported here $\theta_c=0$ but the formulas are given explicitly for $\theta_c\neq 0$.

The average value of $p_n\cos\theta$ may be written

$$\langle p_n\cos\theta\rangle_{Av}=\frac{\int_0^\infty dp\int_0^{\pi/4}d\psi pM(p,\psi)\cos[\theta(p,\psi)]\Theta(\psi)}{\int_0^\infty dp\int_0^{\pi/4}d\psi M(p,\psi)\Theta(\psi)}, \quad (6)$$

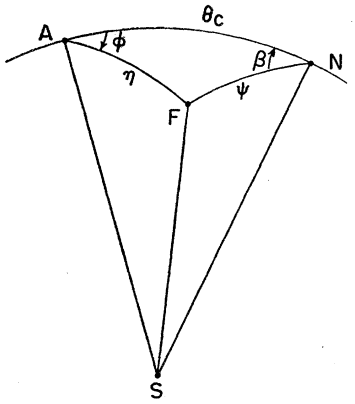

FIG. 11. Spherical triangle used in the calculation of the recoil correction.

where $M(p,\psi)$ is the number of neutrons of momentum p in the c.m. system which emerge at an angle ψ in the laboratory system, and $\Theta(\psi)$ is the distribution of fission fragments in the cone defined by the collimator.

The functions $M(p,\psi)$ were calculated[1] on the basis of isotropic emission, in the c.m. system, of neutrons with an energy spectrum consistent with the observed laboratory spectrum. The distribution of fragments emerging from the collimator is readily calculated in terms of hole dimensions and the angle η,[8] then expressed in terms of ψ. Let $\Omega(\eta)$ be the density of fragments at an angle η. The number in the element of area dA is then

$$\Omega(\eta)dA=\Omega(\eta)\sin\eta d\eta d\varphi=\Omega(\eta)\frac{\sin\eta}{\sin\theta_c\sin\beta}d\eta d\psi. \quad (7)$$

The number between ψ and $\psi+d\psi$ is

$$\Theta(\psi)d\psi=\left\{2\int_{\eta=\theta_c-\psi}^{\eta_{\max}}\Omega(\eta)\frac{\sin\eta}{\sin\theta_c}\times\left[1-\left(\frac{\cos\eta-\cos\psi\cos\theta_c}{\sin\psi\sin\theta_c}\right)^2\right]^{-\frac{1}{2}}d\eta\right\}d\psi. \quad (8)$$

The upper limit, $\eta_{\max}$, of integration is the maximum angle from the axis at which a fragment may emerge from the collimator.

APPENDIX II

Calculation of Frequency of Fission and the Average Total Kinetic Energy as Functions of the Mass Ratio[9]

The experimental data are obtained in the form of frequency of events on a grid whose coordinates are the channel numbers of the recorder chart scale. It is desired to calculate directly from the data the frequency of fission and the average total kinetic energy as functions of the mass ratio and to evaluate the statistical accuracy of the results.

The symbols used are the following:

$x=E_H=$heavy-fragment channel number,

$y=E_L=$light-fragment channel number,

$z=y/x=E_L/E_H=M_H/M_L=$mass ratio,

$g(z)=$frequency of fission,

$E(z)=$average total kinetic energy,

$N=$total number of events,

$\nu(x,y)=$number of events at (x,y), and

$\eta=$transformation variable.

For the frequency distribution one may write

$$g(z)=\frac{1}{N}\int\nu(x,y)\frac{\partial(x,y)}{\partial(\eta,z)}d\eta. \quad (9)$$

Putting $\eta=y$, one gets

$$g(z)=\frac{1}{Nz^2}\int\nu\left(\frac{\eta}{z},\eta\right)\eta d\eta\approx\frac{1}{Nz^2}\sum\nu(x,y)y\Delta y, \quad (10)$$

where the integral is approximated by the summation of the integrand, whose values in the intervals Δy are obtained from the experimental data.

In a similar manner the average total kinetic energy is approximately

$$E(z)\approx\frac{1+z}{Nz^3g(z)}\sum\nu(x,y)y^2\Delta y. \quad (11)$$

The rms error in $g(z)$ due to the combined standard errors $\delta\nu(x,y)$ is given by

$$\langle\Delta g(z)\rangle_{\rm rms}=\{\sum(y\delta\nu\Delta y)^2\}^{\frac{1}{2}}/Nz^2. \quad (12)$$

$E(z)$ is the quotient of two sums, each of which carries the errors in the values of $\nu(x,y)$. The rms error here is

$$\langle\Delta E(z)\rangle_{\rm rms}=\frac{1+z}{z\sum(\nu y\Delta y)}\{\sum[(y^2\delta\nu\Delta y)\sum(\nu y\Delta y)-(y\delta\nu\Delta y)\sum(\nu y^2\Delta y)]^2\}^{\frac{1}{2}}. \quad (13)$$

[8] J. Howlett and W. J. Whitehouse, British Atomic Energy Research Establishment Report N/R 473 (unpublished).

[9] The authors are indebted to Dr. T. D. Newton of this laboratory for suggesting this method of treating the data.